Adaptive Antenna Array Diversity for W-CDMA

DoCoMo is researching the adaptive antenna array diversity technique to further increase the capacity of W-CDMA systems.

This paper reports on the basic configuration of adaptive antenna array diversity and the results of laboratory and field experiments to demonstrate its effectiveness in suppressing interference from other users.

Mamoru Sawahashi, Shinya Tanaka, Taisuke Ihara and Atsushi Harada

1. Introduction

W-CDMA (Wideband Code Division Multiple Access) has been adopted as the radio access scheme for IMT-2000 (International Mobile Telecommunications-2000) [1]～[3]. Because all users communicate using the same frequency band in W-CDMA, the system capacity is to a large extent determined by the level of interference from other users, i.e., MAI (Multiple Access Interference) and interference from delayed path in MPI (Multi-Path Interference). Thus, reducing MAI and MPI by using interference canceller [4], adaptive antenna array diversity [5][6], etc., would increase system capacity. These technologies are being investigated experimentally to test their applicability to W-CDMA systems [7]～[11].

An interference canceller (multi-user detector) used for BS (Base Station) reception increases system capacity by reducing uplink MAI and MPI. It also reduces the required transmit power of the MS (Mobile Station). However, use of an interference canceller in downlink MS reception is not very realistic because it increases the size of the hardware.

High-rate services, such as data downloading from the Internet and broadcasting, are expected to be supported in IMT-2000, meaning that traffic demand will be higher over downlinks than uplinks. Downlink MAI can be reduced by orthogonalizing the channels in the same path with different spreading factors, and thus different symbol rates, by using hierarchical orthogonal code allocation [12]. However, reducing MPI, particularly from high-rate users using high transmit power, should further increase system capacity.

Adaptive antenna array diversity increases antenna gain (directivity) in a particular direction : the number of antennas in the array is set and signal processing is used to adaptively control weight of each antenna, as shown in Figure 1. An adaptive antenna array diversity transceiver is installed in the BS, and the uplink signals received by the antennas are multiplied by optimum antenna weights and then combined. As a result a beam, pattern is generated such that there is a main lobe in the direction of the desired signal and beam nulls in the of arrival of interference signals. SIR (Signal to Interference Power Ratio) of the desired received signal can thus be maximized (Figure 2). The MAI is thereby reduced, leading to an increase in uplink system capacity. Furthermore, in the downlink, it is possible to transmit with increased directivity towards the target user and to reduce interference in the direction of other users by calibrating (as explained later) the received antenna weights and multiplying the weights by the transmission signals to be sent to each user. The downlink system capacity is thereby increased.

This paper explains the configuration for CAAAD (Coherent Adaptive Antenna Array Diversity) reception [13], wherein antenna weights are set to minimize the MSE

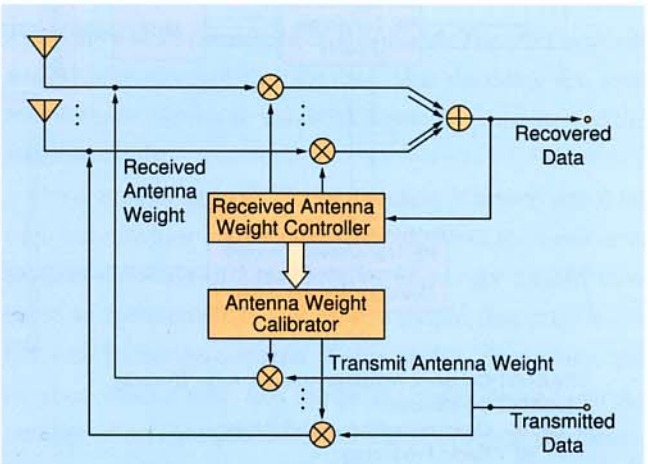

Figure 1 Configuration of Adaptive Antenna Array Diversity

(Mean Squared Error) after Rake combining using decision-directed data symbols and pilot symbols after de-spreading as reference signals. It also explains the configuration for AAA (Adaptive Antenna Array) transmit diversity [8], [10] using the transmit antenna weights generated from the received antenna weights in the CAAAD receiver. It presents the results of laboratory experiments using a fading simulator and field experiments and discusses tasks remaining to achieve practical utilization.

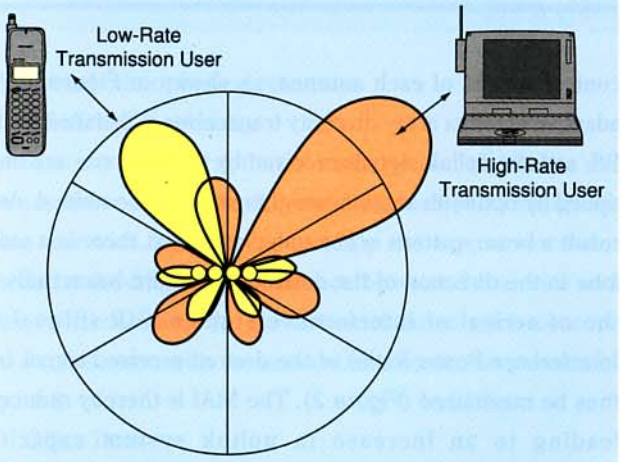

Figure 2 Example of Generated Beam Pattern Using Adaptive Antenna Array Diversity

2. Adaptive Antenna Array Diversity

The adaptive antenna array diversity explained here is an adaptive reception (uplink) and adaptive transmission (downlink) processing technique for the BS. It is applicable to the W-CDMA radio interface [14] being standardized in the 3GPP (3rd Generation Partnership Project). Its use entails simple changes to the processing in a BS device [15] using MF (Matched Filter) Rake combining, which is due to be used when W-CDMA service is introduced. No changes to the MS are required.

Calibrating the received antenna weight generated in the BS receiver generates the transmit antenna weight.

① RF (Radio Frequency) circuitry is calibrated to compensate for the phase and amplitude deviations between the RF transceiver circuitries.

② The carrier frequency is calibrated to compensate for shifts in the direction of the main lobe and in the direction of beam null due to the difference between the uplink and downlink carrier frequencies, which can occur in the DS (Direct-Spread) mode of the FDD (Frequency Division-Duplex) mode.

A block diagram of a BS using adaptive antenna array transmission and reception diversity is shown in Figure 3. For simplicity, it represents for the case of 2antenna and

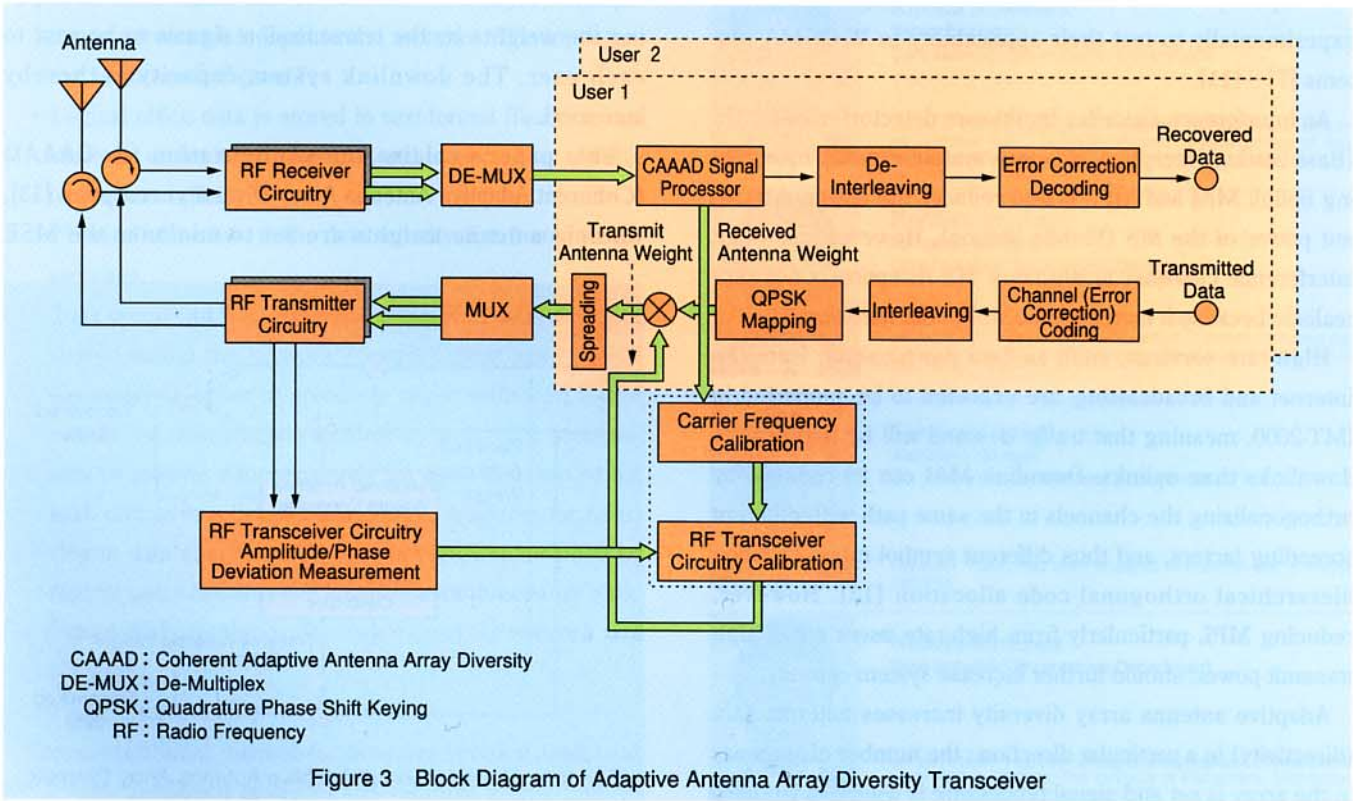

Figure 3 Block Diagram of Adaptive Antenna Array Diversity Transceiver

2user. The uplink signals received by each antenna are amplified and filtered in the RF receiver circuitry, after which received signals at antennas are weighted and combined in the CAAAD receiver. Next, the amplitude and phase variations due to fading of the respective paths are estimated (channel estimation), and Rake combining is performed. After Rake combining, the signal is de-interleaved and decoded to recover the transmitted data. In the BS transmitter, the signal to be sent is channel (error-correction) coded, interleaved, and QPSK (Quadrature Phase Shift Keying) data mapped, and the resulting in-phase (I) and quadrature (Q) components are multiplied by complex-valued transmit antenna weights. Next, the signal is spread, the frequency is converted, and the signal is amplified in the RF transmitter. Finally, the signal is transmitted.

As can be seen from Figure 3, the received antenna weight generated in the CAAAD receiver is affected by the direction of arrival and average reception power of the desired signal and interference signals at the antennas, as well as by amplitude/phase variation in the RF receiver circuitry. Furthermore, the transmit antenna weight generated in the base-band signal processor is affected by the amplitude/phase variation of the RF transmitter circuitry. Thus, to generate received antenna weights that reflect only the arrival direction and average power of the signal received at the antenna, the amplitude/phase variation between the RF receiver circuitries must be removed from the antenna weights which are generated by using the minimum mean squared error (MMSE) algorithm. The ideal complex-valued antenna weight, $W_{ideal}^{(j)}$, (i.e., that corresponding to when $X_{RX}^{(j)}=1$) is expressed by the following equation, where $X_{RX}^{(j)}$ is the complex-valued transfer function of the RF receiver circuitry from the low-noise amplifier of the jth receiver ($1 \leqq j \leqq J$, J = number of antenna elements in the array) until after compensation of the control voltage of the AGC (Automatic Gain Control) amplifier.

$$W_{ideal}^{(j)} = W_R^{(j)} X_{RX}^{(j)} \quad (1)$$

The $W_R^{(j)}$ is the complex-valued receive antenna weight generated in the CAAAD receiver. The antenna weight produced by equation (1) requires compensation for the effect of the transfer function of the RF transmitter circuitry in the base-band transmitter beam-forming processing stage. The transmit antenna weight, $W_T^{(j)}$, to be generated in the AAA transmit diversity is derived from the following equation, where $X_{TX}^{(j)}$ is the transfer function of the jth RF transmitter circuitry.

$$\begin{aligned} W_T^{(j)} &= W_{ideal}^{(j)} / X_{TX}^{(j)} \\ &= W_R^{(j)} (X_{RX}^{(j)} / X_{TX}^{(j)}) \end{aligned} \quad (2)$$

By calibrating the transfer function of the RF receiver and transmitter circuitry to the received antenna weight generated in the CAAAD receiver, as shown in equation (2), it is possible to generate transmit antenna weights that create nulls in the direction of arrival of interference signals received at the antenna.

A block diagram of the CAAAD receiver is shown in Figure 4. The received antenna weight generated in the uplink is used as the transmit antenna weight in the downlink, so there is functional division between the adaptive antenna array and the Rake combiner. Specifically, the beam pattern generated by the adaptive antenna array does not track instantaneous channel variations, but is controlled to maximize the average SIR. The Rake combiner follows the beam former ; it maximizes the instantaneous SIR by weighting and combining the fading reception envelope. The CAAAD receiver is comprised of MFs, a digital beam former, a coherent rake combiner, and an antenna weight controller.

The received signal sequence of each antenna branch is de-spread using a spreading code replica synchronized with the estimated multi-path reception timing for each user. The de-spread signal is weighted and combined using the received antenna weight, and the channel of the resulting signal is estimated using pilot symbols. This estimated value is used to compensate for the phase variation due to fading of the data symbols of each path, and the signal is combined as MRC (Maximum Ratio Combining) is performed. In the antenna weight controller, an adaptive algorithm is used to update the received antenna weight so that the MSE of the signal after Rake combining is minimized. The pilot symbols and decision-directed data symbols after decoding are used as reference signals to establish faster convergence of the antenna weight.

Generating beam nulls in the direction of arrival signal for each low-rate user is practically difficult. First, the number of antenna elements that can be arrayed is very limited compared to the number of voice-transmission (low-rate) users that can be accommodated in one sector. Secondary, the number of beam nulls that can be generated depends on the number of arrayed antenna elements. Consequently, beam-pattern generation in the CAAAD receiver places priority on generating beam nulls in the direction of arrival of signals

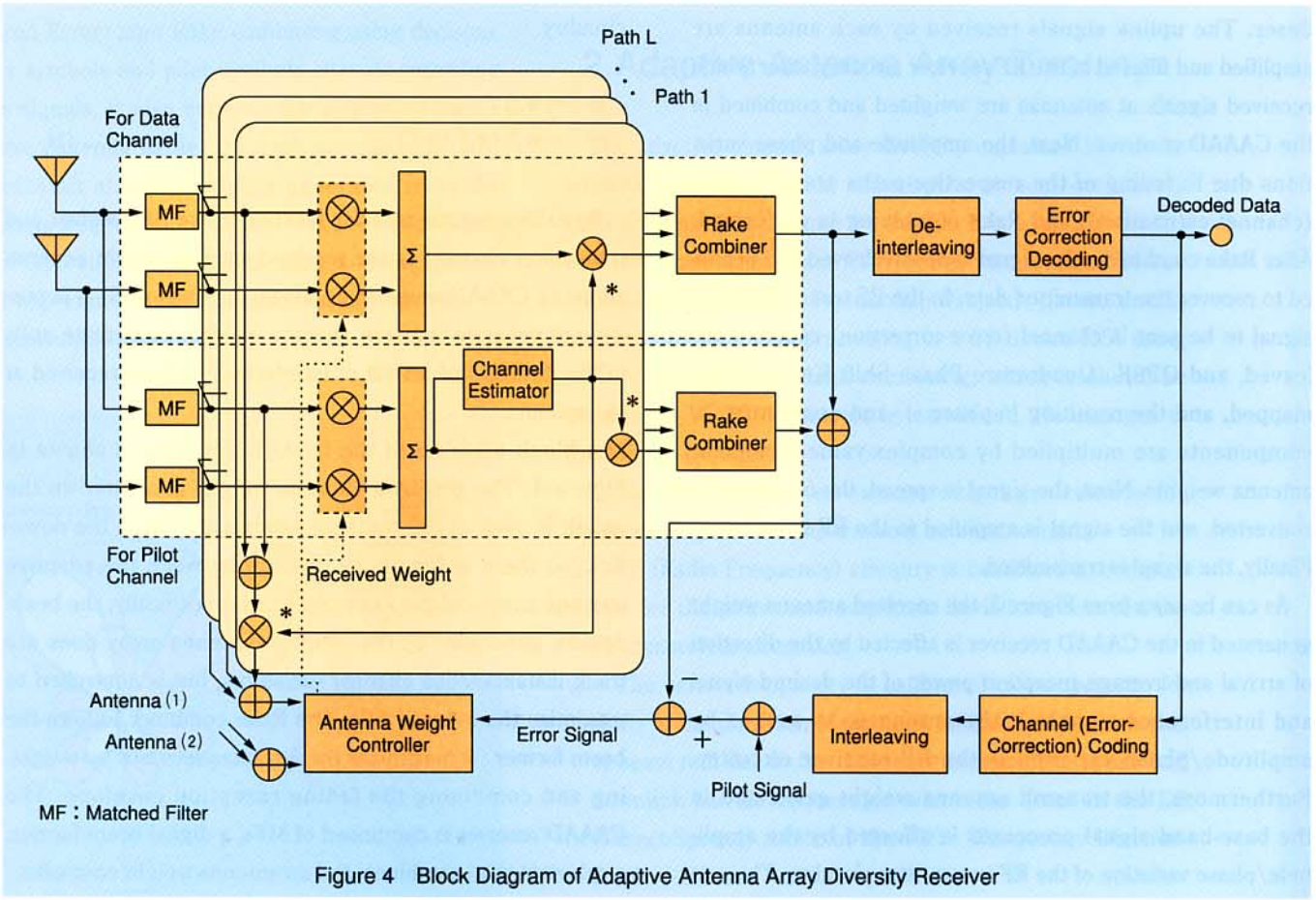

Figure 4 Block Diagram of Adaptive Antenna Array Diversity Receiver

with high transmit power from high-rate users.

Downlink reception quality for low-rate users mainly depends on the extent to which interference from other users (especially high-rate users) can be reduced (Figure 2). Thus, fast TPC (Transmit Power Control) based on SIR measurement is used in the downlink to reduce interference from high-rate users. Specifically, transmission to low-rate users is done using transmit antenna weights that generate beam nulls in the direction of high-rate users. As a result, the interference towards the high-rate users due to the presence of many low-rate users is reduced, such that the high-rate user's transmit power can be reduced using fast TPC. A high-rate user can further reduce transmit power by utilizing the antenna weight with directivity toward his/her own channel. As a result, the high-rate user's transmit power, and thus interference in the direction of low-rate users, can be reduced, such that system capacity is increased.

3. Experimental Results

3.1 Experimental Configuration

The major-radio link parameters of the experimental transceiver are shown in Table 1. The parameters were the same as those used in Ref [16]. The chip rate was 4.096Mcps. The configurations of the BS and MS transmitters will be explained together as they are the same except that in the case of the BS one, the transmit antenna weight is multiplied by the I/Q signals prior to spreading. The data bit rate was 32kbit/s, and convolutional coding with a rate of 1/3 and a constraint length of 7 was used for channel coding. The interleaving size was 1frame (10ms). Each frame comprised 16slots of 0.625msec each, and the symbol rate was 64k symbol/sec (ksps).

After interleaving, the information data sequence was converted to a QPSK symbol sequence, after which four pilot symbols for channel estimation for coherent detection are time multiplexed in front of the 36 information data symbols in each slot. The framed I/Q data sequence is multiplied by the transmit antenna weight for each antenna branch, which is generated by the AAA transmit diversity, and the signal is spread. SF (Spreading Factor) was 64, so the PG (Processing Gain) was 96 (=64x 0.5x 3 ; QPSK mapping is 0.5 and the increase in bandwidth due to convolution coding is 3). A double spreading code consisting of an orthogonal Gold code with a repetition period of 64chips and a scrambling code with a repetition period of 640x 229chips (uplink) or

Table 1 Radio Link Parameters

Chip Rate (Spreading Bandwidth)		4.096 Mcps (5MHz)
Carrier Frequency (Uplink/Downlink)		1990.5/2175.0MHz
Symbol Rate		64ksps
Spreading Factor		64
Data Bit Rate		32kbit/s
Spreading	Spreading Code	Orthogonal Gold Code (64chips/symbol)
	Scrambling Code (Uplink/Downlink)	Gold Code (cut at a specified length) (640×2^{29}chips/40960chips)
Modulation	Data	QPSK (Quadrature Phase Shift Keying)
	Spreading	QPSK
Channel Estimation		Channel Estimation using Pilot Symbols (two-slot average)
Channel Coding/Decoding		Convolutional Code (r=1/3, K=7) Soft-decision Viterbi Decoding
Interleaving Length		10ms

40960chips (downlink) was used. The spread data was confined within a 5MHz bandwidth using a root nyquist filter with a roll-off factor (α) of 0.22, converted to a carrier frequency of 1990.5MHz in the uplink and 2175MHz in the downlink, amplified with a power amplifier, and transmitted.

The received signals were frequency dawn converted and liner amplified by AGC. Then, the IF (Intermediate Frequency) signals were converted into base band I/Q components by the quadrate detector. After quadrate detection, the I/Q components were converted into a digital signal using an 8-bit A/D converter with a sampling rate (16.384MHz) four times the chip rate, after which bandwidth filtering was done using a root nyquist filter. The resulting signal was input to the CAAAD receiver. The Rake combined-signal output from the CAAAD was de-interleaved, then soft-decision Viterbi decoded.

The power delay profile was measured using a sector antenna (of the four antennas, one had a reception weight of 1 and the others had a reception weight of 0). Based on the measured delay profile, the three paths with the highest reception power exceeding a threshold value were used as the paths for Rake combining. The average time for generating the delay profile and updating the time for multi-path selection for Rake combining was 100msec. The received antenna weight for each path was updated in the weight controller using a N-LMS (Normalized Least Mean Square) algorithm so that the MSE of the signal after Rake combining was minimized. (The pilot symbols and tentative decision data symbols after rake combining were used as a reference signal to expedite received antenna weight convergence). The equation for updating is given in Ref [8]. In our experimental equipment, weight updating was carried out every four symbols (62.5 μ sec) using a step size (μ) of 10^{-4}.

3.2 Laboratory Experiments

The effect of adaptive antenna array diversity reception was first evaluated by laboratory experiment. Transmitted signals were input to a hardware simulator that generated rayleigh fading of two paths with no correlation between them. In an actual propagation environment, signals from different users would arrive at each antenna from somewhat different directions. However, it was assumed that there was sufficiently far distance between the MSs and the BS, so that the arrival angle at all antennas was the same (i.e., the carrier could be considered a plane wave). The variance in arrival angles of each of the rayleigh fading paths was ignored (it was assumed that inter-antenna fading correlation, ρ, was 1). It was assumed that the delay-time difference between 2paths was 0.3 μ sec (corresponding to 1.23chips) and that the arrival angle of the 2paths was the same (i.e., the variance of angle α was 0). Thus, the signals received at antenna j differed only in phase from the signals received at the other antennas. This phase difference is given by the following equation.

$$\psi_j = 180 \times (j-1) \sin\theta \qquad (3)$$

Here, θ represents the angle of arrival, and it is assumed that the antennas are arranged linearly with separation of half a carrier wavelength. The two-path Rayleigh fading waves were divided into four, after which the phase difference given by equation (3) based on the arrival direction for each antenna was added by the phase shifter, and the resulting signal was combined with the signals from the other users. Gaussian noise was also added to the receiver.

The received antenna beam patterns are shown in Figure 5 after convergence of the first path of the desired user (user 1) when there were four antennas and the number of users was two (one interference user) (Figure 5(a)) or six (five interference users) (Figure 5(b)). The direction perpendicular to the antenna array was 0°, and the arrival angles of the signals from user 1 and user 2 were −50° and +40°, respectively. The initial weight was 1 for antenna 1 only and 0 for all other antennas. The average received SIR was −15dB for the desired signal at the BS. The average received

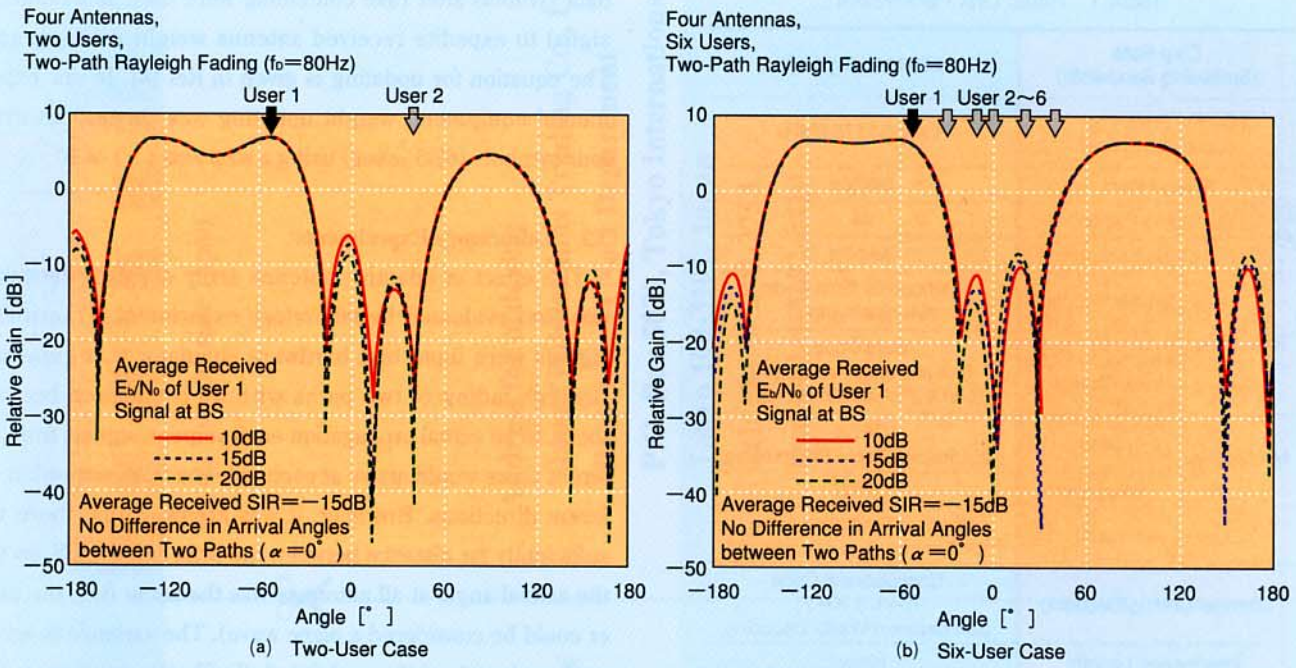

Figure 5 Generated Received Beam Pattern with Average Received E_b/N_0 as a Parameter

E_b/N_0 (where N_0 is the background noise power density of the receiver) was used as a parameter. The figure shows that a beam pattern with a beam null in the direction of arrival of the interference signals was generated (the direction of the null was off by less than 3°). Furthermore, it is evident that the greater the average received E_b/N_0, the deeper the null. In the case of the six-user environment, although the number of interference users was greater than the number of nulls that could be generated, approximately 15dB interference suppression was achieved in the direction of the desired user.

The average BER (Bit Error Rate) performance is shown in Figure 6 as a function of average received SIR. The average received E_b/N_0 for the desired user as a parameter. For comparison, the results when SD (Space Diversity) with four branch MRC are also shown (for $\rho = 0$ and 1). Clearly, the BER performance can be greatly improved compared to SD reception when interference power is high. For example, when the average received E_b/N_0 was 10dB and the average received SIR was −20dB, the average BER was 10^{-4} in the case of CAAAD reception, whereas in the case of SD reception, the average BER was 10^{-2} even when ρ was 0. (The spacing between antennas was half a carrier wavelength for CAAAD reception, so the antenna spacing would have to be several carrier wavelengths or more to make $\rho = 0$ in the BS in the case of SD reception).

Furthermore, it can be seen that CAAAD reception can

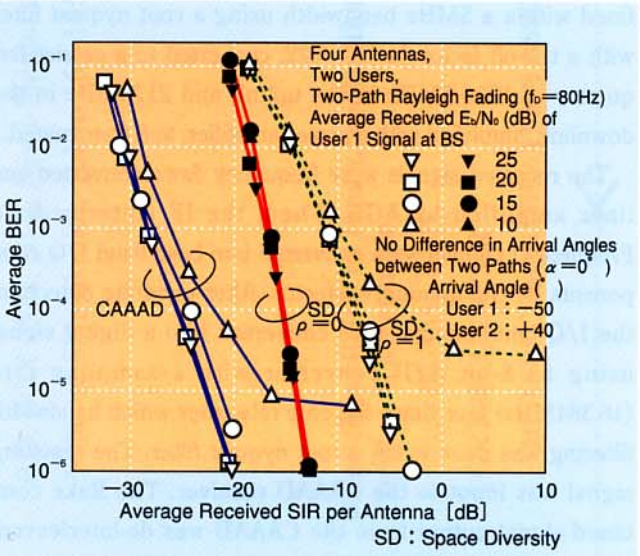

Figure 6 Average BER Performance as a Function of Average Received SIR

achieve average a BER of 10^{-3} at an interference signal power 10dB greater than in the case of SD reception. CAAAD reception is thus effective for reducing interference from other users transmitting at a high rate at high transmit power. This is because interference power can be greatly suppressed by directing a beam null in the direction with the highest interference power, as apparent from Figure 5. This improves the received SIR. The improvement in CAAAD reception compared to SD reception was about the same regardless of SIR level when ρ was 1. However, when ρ was

0, the improvement decreased as the SIR increased. This is because the antenna array is only used to generate null beams in the case of CAAAD reception (and thus there is no space diversity effect) while in the case of SD reception, the diversity effect for thermal noise increases as the fading correlation approaches zero.

As stated above, the performance of CAAAD reception is degraded more than those of SD reception in a low-interference, noise-limited environment because CAAAD reception lacks the space diversity effect. By using fast TPC to keep the received signal level constant, it is possible to reduce the degradation in reception performance caused by fading variation. The required relative transmit power for the average BER of 10^{-3} at maximum Doppler frequency f_D using fast TPC and two antennas is shown in Figure 7. The performances are given using the average received SIR of the desired signal at the BS as a parameter. For comparison, the performance for SD reception ($\rho = 0$) using MRC are also shown. The relative average transmit power is expressed such that the MS's average transmit power required to achieve a BER of 10^{-3} using fast TPC with one user and one antenna reception is 0dB. The required average transmit power was approximately the same over a broad range of f_D due to the increased effect of fast TPC in the slow fading range up to $f_D \leqq 300$Hz (corresponding to 150km/h in the 2GHz band) and of interleaving and channel coding in the fast fading range. The required transmit power increased in the range $f_D \geqq 300$Hz because channel estimation using pilot symbols has difficulty keeping up with fading variation. As can be seen from the figure, the required average transmit power for the average BER of 10^{-3} at $f_D \leqq 500$Hz when the average received SIR is −9dB can be reduced approximately 2dB with CAAAD reception as compared to SD reception. The required average transmit power can be reduced as much as 4-7dB when the average received SIR is −12dB. CAAAD reception greatly reduced interference power when the interference power was high, whereas fast TPC compensated for the effect of fading when the interference power was relatively low and the effect of background noise could not be ignored. Therefore, CAAAD reception used jointly with fast TPC achieves a greater overall improvement in performances than SD reception.

Next, AAA transmits diversity performances were evaluated in a downlink using four antennas. Figure 8 shows an example of beam patterns generated at the antenna with and without RF transmitter circuitry calibration. The carrier frequency calibration was not conducted. The average received

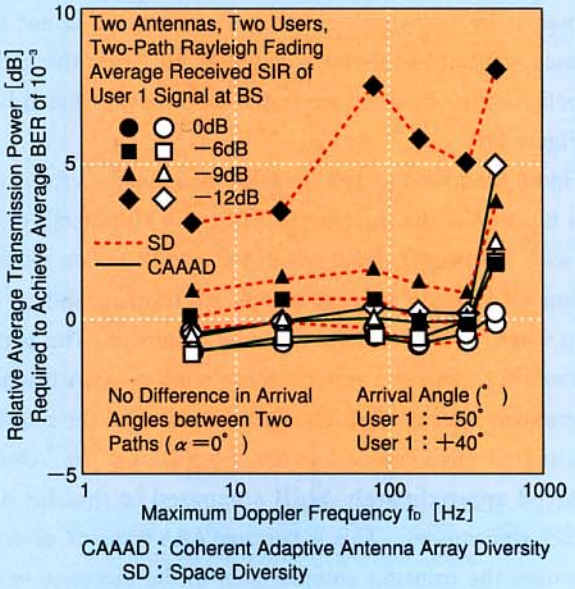

Figure 7 Required Relative Average Transmit Power for the Average BER of 10^{-3} Using Fast TPC as a Function of f_D

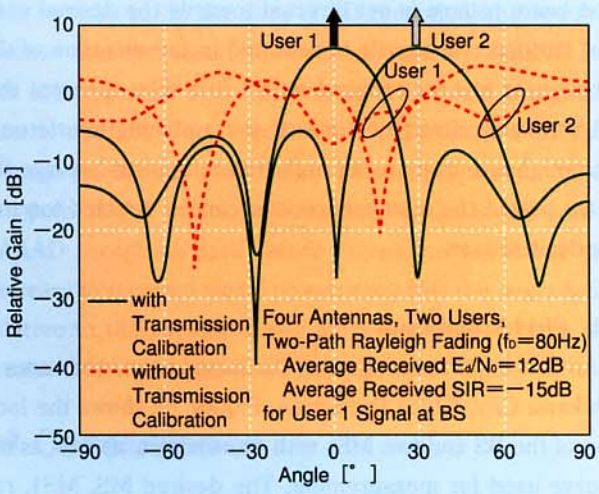

Figure 8 Generated Beam Transmit Pattern

E_b/N_0 was 12dB, and the average received SIR was −15dB at the BS for the signal of user 1. The directions of arrival of the signals from users 1 and 2 were set at 0° and +30°, respectively. The forward and, reverse link carrier frequencies differed because an FDD system was used. However, the null of the generated transmission beam pattern shifted only approximately 3° from the direction of the interference user (user 2) because the difference between the forward and reverse link carrier frequencies was only approximately 9.3% of the reverse link carrier frequency. By applying RF circuitry calibration to the received antenna weights, it is possible to generate transmitted antenna weights main lobe towards

the desired signal and a beam null towards the interference signal. If RF transmitter circuitry calibration is not performed, the null shifts approximately 50° from the arrival direction of the interference signal (shown with dotted lines in Figure 8).

Figure 9 shows the average BER performances for user 1 as a function of the transmitted SIR (ratio of transmit power for user 1 versus transmit power for user 2) before multiplication by antenna weights during BS transmission in the case where AAA transmits diversity is applied. The performances for 1antenna transmission without AAA transmit diversity are also shown. The figure shows that the required transmitted SIR for user 1 to achieve a BER of 10^{-3} can be reduced approximately 14dB compared to that for one-branch transmission. This is because AAA transmit diversity improves the transmit antenna gain in the direction of the desired user while reducing the strength of the interference signals transmitted towards the desired user. The BER performances deteriorate when RF transmitter circuitry calibration is not performed because the main lobe of the transmission beam pattern is not directed towards the desired user, and interference signals transmitted in the direction of the target user are not reduced much. It is thus apparent that AAA transmit diversity is effective in reducing interference from high-rate users using high transmit power because the beam null of the interference user can be directed towards the desired user.

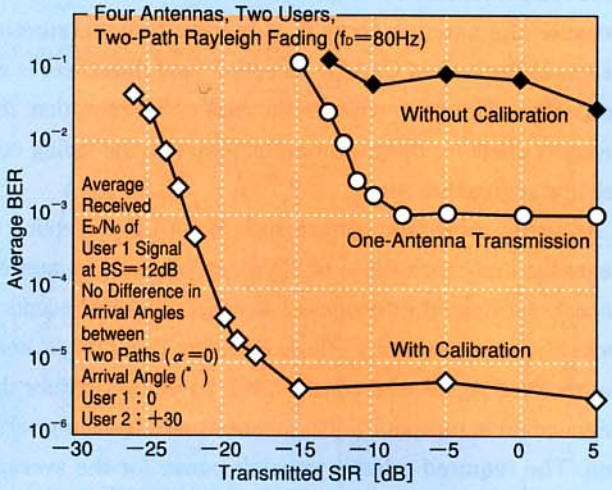

Figure 9 Average BER Performances as a Function of to Transmitted SIR before to Multiplication by Antenna Weight

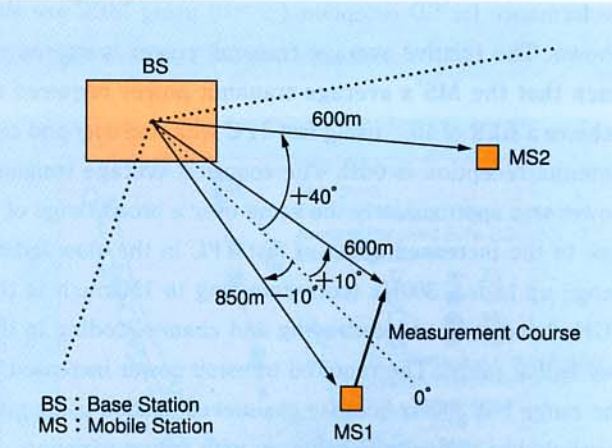

Figure 10 Measurement Course for Field Experiments

3.3 Field Experiments

An field experiment test was conducted in an urban area in Ichikawa City, Chiba Prefecture. Figure 10 shows the location of the BS and two MSs with transceivers, as well as the course used for measurement. The desired MS, MS1, ran the measurement course at an average speed of approximately 30km/h. The distance from points along the measurement course to the BS ranged from about 600 to 850meters, and the position of MS1 in relation to the BS ranged from −10° to +10°. The interference MS, MS2, remained stationary at an angle of +40° to the BS and at a distance of approximately 600meters from the BS. The BS had a linear array of sector antennas at a height of 50meters with 120° beams. The antenna spacing was $\lambda/2$ (λ was the reverse link carrier wavelength) (Figure 11). Both MSs had an antenna height of 2.9meters. The course passed through a low-rise residential area, which created a 2-3-path environment. MS2 was almost in the line-of-sight path. Here we describe the performances exhibited without the use of fast TPC.

The generated beam pattern with four-antenna reception of the uplink signal from MS1 using CAAAD for the path with maximum reception power is shown in Figure 12. While MS1 was running the course, the average received E_b/N_0 per antenna at the BS for the MS1 signal was 25dB, and the average received SIR was −15dB. The direction of the main lobe shifted in response to the change in the arrival direction of the received signal as MS1 moved. Even though MS2 (the interference MS) remained stationary at an angle of +40° in relation to the BS, the position of the beam null shifted in accordance with movement of the MS1. This is thought to be because the received antenna weight converges to maximize the SIR and thus antenna gain in the arrival direction of the desired signal increases, causing the beam null to shift away from the arrival direction of the interference signal.

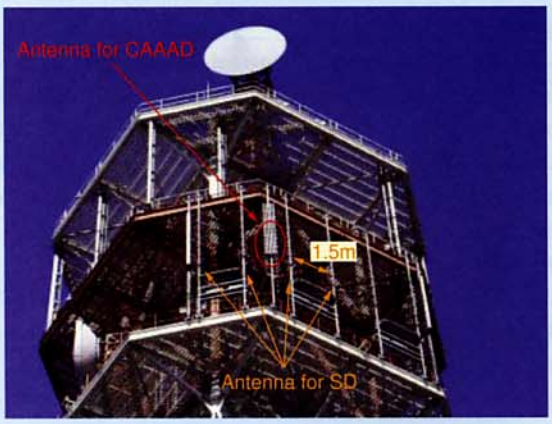

CAAAD : Coherent Adaptive Antenna Array Diversity
SD : Space Diversity

Figure 11 Antenna used for Field Experiments

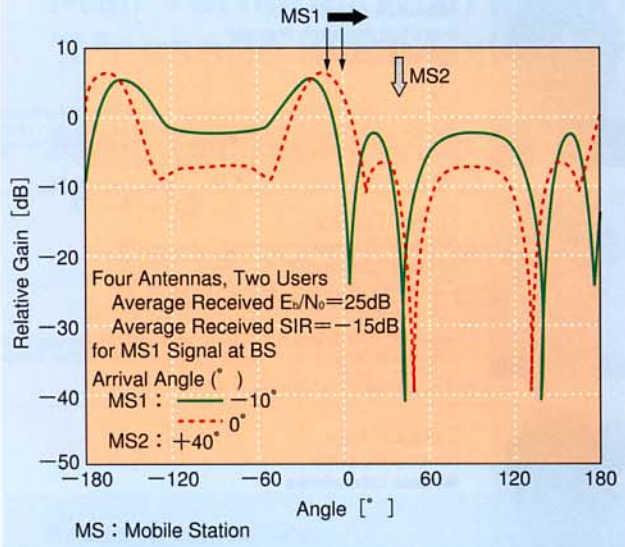

MS : Mobile Station

Figure 12 Generated Received Beam Pattern

The average BER performance is plotted as a function of the average received signal power for CAAAD reception of the MS1 signal at a BS with four antennas is shown in Figure 13. The average E_b/N_0 received at the BS was 25dB and the average received SIR was −12dB, −15dB for each antenna. For comparison, the performances of SD reception (antenna spacing 10λ) using MRC with the same number of antennas are also shown. The use of CAAAD reception made it possible to reduce the required average received power for the average BER of 10^{-3} by 5 to 10dB when the average received SIR was −12dB and by 8 to 10dB when the average received SIR was −15dB, as compared to SD reception. The received antenna weight is apparently able to accurately track the change in the direction of arrival of the signal received by the BS from the desired MS, such that high-reception-power

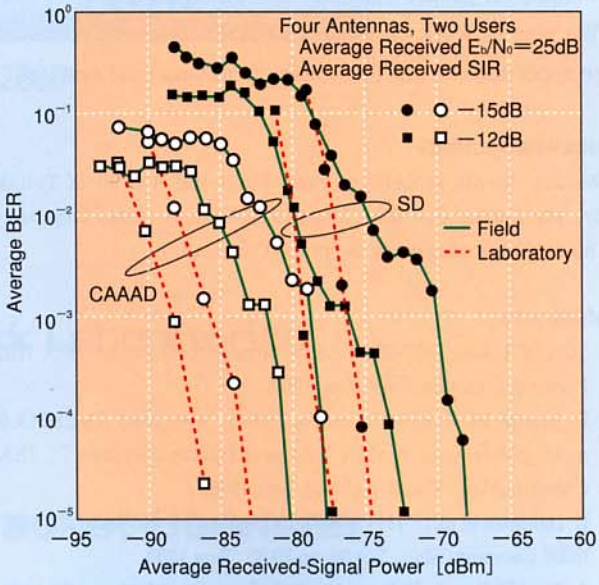

CAAAD : Coherent Adaptive Antenna Array Diversity
SD : Space Diversity

Figure 13 Average BER Performances as a Function of Average Received-Signal Power

MAI is reduced. In the case of SD reception, the required average received signal power for the average BER of 10^{-3} was approximately 1 to 4dB greater in the field experiment than in the laboratory experiment (2path model with equal average power) due to differences in the propagation model and path search errors for Rake combining. In the case of CAAAD reception, path search errors increased due to a decrease in received signal power, such that the degradation relative to the results of the laboratory experiment was greater than in the case of SD reception.

4. Conclusion

This paper described an adaptive antenna array diversity technology that can be used to further increase link capacity in W-CDMA systems and demonstrated its effect in improving reception quality in laboratory and field experiments. Several tasks remain before this technique can become practical.

(1) The BS, including its antennas, RF circuitry, and baseband signal processor must be made smaller.
(2) To save space, an optical fiber should be used as the feeder line between the top amplifier and the indoor equipment.
(3) Methods must be developed for calibrating RF circuitry in commercial systems.
(4) Methods must be developed for generating antenna

weights for packet transmission (bursty signals).

We plan to work on these and other tasks and to investigate application of this technology to commercial systems.

Acknowledgments

We are deeply grateful to Prof. Fumiyuki Adachi of Tohoku University (former Executive Manager of Radio Accesses Laboratory) for his kind advice regarding the present research.

References

[1] Special Issue, IMT-2000 : Standards efforts of the ITU, IEEE Personal Commun.,Vol.4, Aug.1997.

[2] F. Adachi, M. Sawahashi and H. Suda : "wide-band DS-CDMA for next generation mobile communications system", IEEE Commun.Mag., Vol.36, pp.55-69, Sept.1998.

[3] E. Dahlman et al. : "IMTS/IMT-2000 based on wideband CDMA", IEEE Common. Mag., Vol.36, pp.70-80 , Sept.1998.

[4] A. Duel-Hallen, J. Holtzman and Z. Zvonar : "Multiuser Delection for CDMA Systems", IEEE Personal Communications, pp.46-58, Apr.1995.

[5] A.J. Pauraj and B.C.Ng : "Space-Time Modems for Wireless Personal Communications", IEEE Personal Commu. Mag., Vol.5, No.1, pp.36-48, Feb.1998.

[6] R. Kohno : "Spatial and temporal communication theory using adaptive antenna array", IEEE Personal Communication, pp.28-35, Feb.1998.

[7] M. Sawahashi, H. Andoh, K. Higuchi and F. Adachi : "Experiments on Coherent Multistage Interface Canceller for DS-CDMA Mobile Radio", Proc. PIMRC '98, pp.491-496, Boston, U.S.A, Sept.1998.

[8] S. Tanaka, A. Harada, M. Sawahashi and F. Adachi : "Transit diversity based on adaptive antenna array for W-CDMA for word link", Proc. CIC '99, pp.282-286, Seoul, Korea, Oct.1999.

[9] Tanaka, Harada, Ihara, Sawahashi, Adachi : "Field experiment coherent adaptive antenna array diversity receiver for W-CDMA receiver link, "IEICE Technical Report RCS99-130, pp.45-50, Oct.1999.

[10] Harada, Tanaka, Sawahashi, Adachi : "The effect of the calibration of phase and amplitude variation of the transmitter/receiver RF circuit for DS-CDMA adaptive antenna array transmit diversity," 1999 IEICE Conference in Spring, B-5-165, pp.516, Mar.1999.

[11] A. Harada, S. Tanaka, M. Sawahashi and F. Adachi : "Performance of Adaptive Antenna Array Diversity Transmitter for W-CDMA Forward Link", Proc. PIMRC99, pp.1134-1138, Osaka, Japan, Sept.1999.

[12] K. Okawa and F. Adachi : "Orthogonal forward link using orthogonal multispreading factor codes for coherent DS-CDMA mobile radio", IEICE Trans. Commun., Vol.E81-B, pp.777-784, Apr.1998.

[13] S. Tanaka, M. Sawahashi and F. Adachi : "coherent adaptive array diversity for DS-CDMA mobile radio reverse link", IEICE Trans. Fundamentals, Vol.E80-A, pp.2445-2454, Dec.1997.

[14] 3GPP RAN 25.211 V3.1.0, Dec.1999.

[15] "Special Issue on W-CDMA System Experiment (1)" NTT DoCoMo Technical Journal Japanese version Vol.6, No.3, pp.6-29, Oct.1998.

[16] "Specifications of Air-Interface for 3G Mobile System Ver.0.0", Dec.18, 1997, Association of radio Industries and Businesses (ARIB).

[17] S. Haykin, Adaptive Filter Theory, Prentice-Hall, 1991.